Electronic Structures of Bis- and Monothiophene Complexes with Fe, Co, Ni: A Density Functional Theory Study

Yunqiao Ding,[†,‡] Maoxia He,[§] Yuzhong Niu,[†] Dengxu Wang,[†] Yan Cui,[†] and Shengyu Feng*[,†]

School of Chemistry and Chemical Engineering, Shandong University, Jinan 250100, P. R. China, and Environment Research Institute, Shandong University, Jinan 250100, P. R. China

Received: March 31, 2009; Revised Manuscript Received: June 18, 2009

A density functional theory study for the bis- and monothiohene complexes of Fe, Co, and Ni (MT_2 and MT, T = thiophene, M = Fe, Co, Ni) was performed to understand their coordination geometries, bonding properties, vibration spectra and singlet excited state spectra. The typical metal coordination exists in the complexes. The Fe−thiophene coordination has the highest stability, with Ni−thiophene being the second highest, and Co−thiophene the lowest. Bisthiophene complexes of Co and Ni prefer to homolytically dissociate to their monothiophene ones and free thiophene. Frequency calculation shows that the ligand−M−ligand asymmetric stretching vibration in bisthiophene complexes shows a strong absorption, at 435.2, 495.7, and 383 cm^{-1} for Fe(η^4-T)$_2$, Co(η^2-T)$_2$ and Ni(η^2-T)$_2$, respectively. The M−S stretching vibration in monothiophene complexes shows a strong absorption in the far-infrared region, at 209, 156, and 150 cm^{-1} for Fe(η^4-T), Co(η^4-T) and Ni(η^5-T), respectively. The excited state spectra indicate that the characteristic absorption wavelengths of the complexes have a red shift of more than 12.40 eV compared to free thiophene, at 3.54, 1.64, 3.83, 2.75, 1.43, and 2.58 eV for Fe(η^4-T)$_2$, Co(η^2-T)$_2$, Ni(η^2-T)$_2$, Fe(η^4-T), Co(η^4-T), and Ni(η^5-T), respectively.

1. Introduction

The complexes of thiophene with transition metals have been investigated extensively during the past decades to study the mechanism of thiophene hydrodesulfurization on heterogeneous catalysts.[1−5] Recently, much attention has been paid on the metal−thiophene complexes due to their potential application in electronic devices and chemical sensors.[6,7] In the metal−thiophene complexes, the thiophene can coordinate to single metal centers through the sulfur (η^1), two carbons (η^2), four carbons (η^4), and five atoms (η^5) of the thiophene ring, respectively. Various coordination modes enable to produce the metal−thiophene complexes with the diverse geometrical structures. The resulting new supermolecular architectures with various topology structures are the subjects of several interesting and challenging studies.[8−10] As functional materials, new terthiophene-functionalized metal nanotubes have been synthesized by the electropolymerization.[11]

Due to weak coordination in the metal−thiophene complexes, the thiophene ligand can be easily displaced by other ligands, which has been utilized in many organic reactions.[12] The common transition metals that can be strongly bonded to thiophene are those of VIB, VIIB, and VIII metals.[4,13,14] The thiophene complexes with Fe, Co, and Ni have been employed in many catalysis reactions, while the isolable complexes are difficult to obtain.[12] It is well-known that the materials based on Fe, Co, and Ni are useful in the field of the high density magnetic recording materials,[15] the wave-absorbing and radar-resisting materials,[16] the highly effective and cheap catalysts,[17,18] and so on. The thiophene-based heteroaromatic compounds also exhibit the novel photoelectric properties in the application of the electronic devices.[19−22] Accordingly, the bonding properties and stability of thiophene complexes with Fe, Co, and Ni are of great interest. Previous documents reported many studies of the aromatic complexes in experiment and theory, such as pentazolato complexes with the first row transition metals,[23] sandwich complexes $[Ti(\eta^5\text{-}E_5)_2]^{2-}$ (E = CH, N, P, As, Sb).[24] However, there is a little theoretical research on the thiophene complexes as well as on the description of metal−thiophene bonding properties, especially for the complexes of Fe, Co, Ni.

Present study aims at the quantum chemical calculation of thiophene complexes with Fe, Co, Ni, and discusses their geometrical structures, bonding properties, stability, vibrational and excited state spectral properties to understand the relationship between structures and properties, and design new thiophene-based chemical species. The study is expected to provide the new insight into the applications of thiophene complexes in the exploitation of new catalysts with low cost and high reactivity, nanoelectrochemistry, chemical/biological separation, supramolecular self-assembly, sensor developments, and so on.

2. Computational Methods

The Becke's 3-parameter hybrid functionals combined with the Lee−Yang−Parr correlation functional method (B3LYP)[25−27] of density functional theory (DFT)[28,29] were employed to optimize the ground state geometries of neutral metal−thiophene complexes with the 6-31+G(d) basis sets,[30] followed by the calculation of vibration frequencies. The spin multiplicities of the complexes were singlet for Fe and Ni complexes, and doublet for Co complex, respectively. The dissociation enthalpies of metal−thiophene coordinate bonds, ΔH, were calculated at the B3LYP/6-31+G(d) level of theory by the following equation:

* Corresponding author. Tel.: +86-531-88364866. Fax: +86-0531-88564464. E-mail: fsy@sdu.edu.cn.
† School of Chemistry and Chemical Engineering.
‡ E-mail: dyq@sdu.edu.cn.
§ Environment Research Institute.

10.1021/jp902920w CCC: $40.75
Published on Web 08/27/2009

$$\Delta H = \sum E_{\text{fragments}} - E_{\text{complex}} + \Delta E_{\text{cp}}$$

where $\Sigma E_{\text{fragments}}$ is the sum of energies of specified fragments dissociated from relevant complex (see below eqs i−v); E_{complex} is the energy of the complex composed of the specified fragments; ΔE_{cp} is the counterpoise correction (CP)[31−33] energy, which is to handle the basis set superposition error.[34,35] The computed energies were corrected to constant pressure and 298 K for zero point energy differences, for the contributions of the translational, rotational, and vibrational partition functions. Based on equilibrium geometries, the natural bond orbital (NBO) population analysis[36,37] was carried out using MPWB1K[38,39] method of DFT at the 6-311+G(d,p) basis set level. Time-dependent density functional theory (TD-DFT)[40−43] was used to calculate the first ten singlet excited state energies at TD-MPWB1K/6-311+G(d,p) level of theory. All calculation and simulation were performed using the Gaussian 03 package.[44]

3. Results and Discussion

3.1. Optimized Geometries. Followed by simple potential energy scan, full geometrical optimization for model compounds,

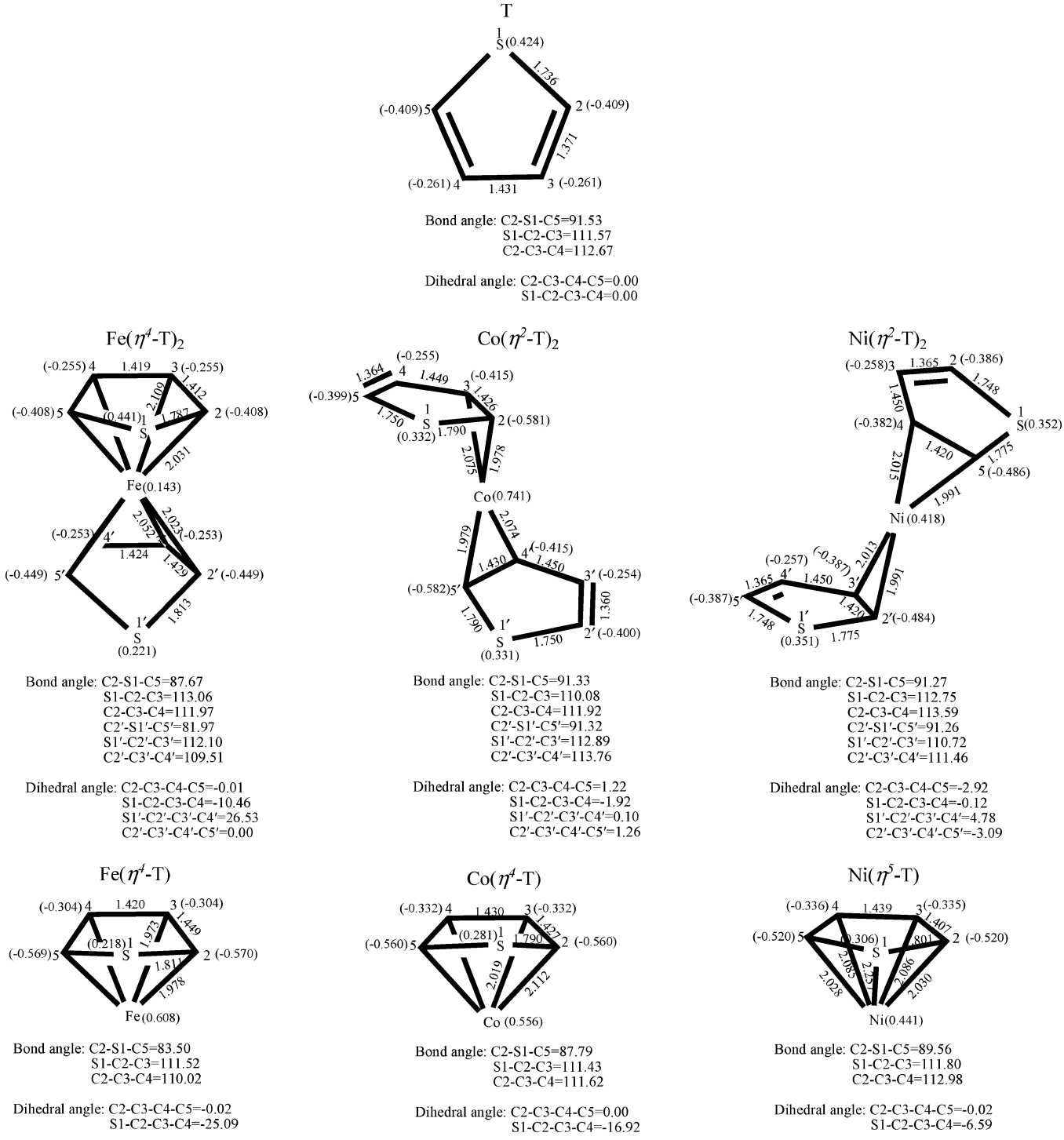

Figure 1. Equilibrium geometries of bis-/monothiophene complexes of Fe, Co, Ni computed at the B3LYP/6-31+G(d) level. All H atoms are hidden. The bond length is in Angstroms and the angle is in Degrees. The data in parentheses are natural charges (in au) calculated at B3LYP/6-31+G(d)//MPWB1K/ 6-311+G(d,p) level.

TABLE 1: Atom−Atom Overlap-Weighted NAO Bond Order Computed at the B3LYP/6-311+G(d,p) Level

BD	T	Fe(η^4-T)$_2$	Co(η^2-T)$_2$	Ni(η^2-T)$_2$	Fe(η^4-T)	Co(η^4-T)	Ni(η^5-T)
S^1-C^2	0.931	0.857	0.857	0.905	0.840	0.878	0.868
S^1-C^5	0.931	0.857	0.897	0.888	0.840	0.878	0.867
$C^2=C^3$	1.282	1.169	1.133	1.305	1.077	1.169	1.226
C^3-C^4	1.068	1.108	1.035	1.029	1.127	1.079	1.082
$C^4=C^5$	1.282	1.169	1.307	1.175	1.078	1.169	1.226
$M-S^1$		0.178					0.104
$M-C^2$		0.208	0.241		0.301	0.191	0.168
$M-C^3$		0.138	0.217		0.211	0.176	0.128
$M-C^4$		0.138		0.206	0.211	0.176	0.128
$M-C^5$		0.208		0.225	0.301	0.191	0.168
$S^{1'}-C^{2'}$		0.818	0.897	0.890			
$S^{1'}-C^{5'}$		0.817	0.858	0.905			
$C^{2'}=C^{3'}$		1.128	1.307	1.174			
$C^{3'}-C^{4'}$		1.087	1.035	1.028			
$C^{4'}=C^{5'}$		1.128	1.131	1.306			
$M-S^{1'}$							
$M-C^{2'}$		0.247		0.226			
$M-C^{3'}$		0.180		0.206			
$M-C^{4'}$		0.180	0.217				
$M-C^{5'}$		0.247	0.241				

bis- and monothiophene complexes (MT_2 and MT; T = thiophene, M = Fe, Co, Ni), was performed at the B3LYP/6-31+G (d) basis set level of theory. Equilibrium geometries were shown in Figure 1, together with the selected geometric parameters. The equilibrium geometries of complexes are stable with no imaginary frequencies, involving the η^5-bonding mode of the thiophene ligand for Ni(η^5-T), the η^4-bonding mode for Fe(η^4-T)$_2$, Fe(η^4-T), and Co(η^4-T), η^2-bonding mode for Co(η^2-T)$_2$ and Ni(η^2-T)$_2$, respectively. The symmetry of thiophene unit in complexes lowers, or disappears due to the coordination effect. The S−C bond lengths in complexes are much longer than those of free thiophene. Four C atoms of each thiophene unit in complexes are nearly coplanar, while there is a folding angle between the $C^2-C^3-C^4-C^5$ and C^2-S-C^5 planes, especially, such angle in Fe complexes is more obvious than that in the others, see Figure 1.

The geometry of Fe(η^4-T)$_2$ shows the metallocene-like structures with the eclipsed (C_s) conformation. The distances between Fe center and the thiophene centroid are 1.920 and 1.617 Å, respectively. At the same calculation level, the distance in ferrocene (Cp_2Fe) between Fe center and the cyclopentadienyl centroid is about 1.710 Å, and the corresponding experimental value is about 1.660 Å.[23] The comparison between Fe(η^4-T)$_2$ and Cp_2Fe indicates that thiophene shows the similar bonding properties to cyclopentadienyl ligand. In Fe(η^4-T)$_2$, the coordination of thiophene to Fe through four carbon atoms results in that the C=C bond length and C−C bond one are close to each other. The distances between Fe and C atoms bonded to S atom (C^2, C^5, $C^{2'}$, and $C^{5'}$) are shorter by 0.077 Å than those between Fe and C atoms nonbonded to S atom (C^3, C^4, $C^{3'}$, and $C^{4'}$). Co(η^2-T)$_2$ and Ni(η^2-T)$_2$ show the zigzag conformation without the symmetry. Compared to free thiophene, in Co(η^2-T)$_2$ and Ni(η^2-T)$_2$, the coordination of thiophene to metal through two carbon atoms causes the lengthening of the coordinated C=C bond as well as the C−C bond, but the shortening of uncoordinated C=C bond, which results from the coordination of the π-orbital of double bond to the empty valence orbital of central metal. And the coordinated distances between the metal and those C atoms bonded to S atom (C^2 and $C^{5'}$) are notably shorter than those between metal and those C atoms nonbonded to S atom (C^3 and $C^{4'}$), about 0.096 ± 0.001 Å for Co(η^2-T)$_2$, and 0.023 ± 0.001 Å for Ni(η^2-T)$_2$, respectively.

The M−C bond distances from the covalent radii of elements are 1.935 Å for Fe−C, 1.930 Å for Co−C, and 1.920 Å for Ni−C, respectively. The computational results show that the M−C bond length in MT_2 becomes longer, as a result of significant interaction between thiophene and metal. The observed bond increases are as much as 0.174 Å for the Fe−C bond, 0.145 Å for the Co−C bond, and 0.095 Å for the Ni−C bond, respectively. The increased M−C bond length in MT_2 is consistent with the weaker interaction in the metal complex, as the bond from the covalent radii represents a stronger direct bonding.

All monothiophene complexes show C_s symmetry, in which each bond length of the thiophene unit is lengthened compared to the free thiophene. The distances between the metal center and thiophene centroid are about 1.655, 1.716, and 1.650 Å for Fe(η^4-T), Co(η^4-T), and Ni(η^5-T), respectively. The Fe−C bond lengths in Fe(η^4-T) are shorter than those in Fe(η^4-T)$_2$, which implies that the M-C bond strength in Fe(η^4-T) is stronger than that in Fe(η^4-T)$_2$. The weakening of interaction between thiophene and Fe with the increasing of ligand indicates the saturation of coordination between them. In sharp contrast, the Ni−C bond lengths in Ni(η^5-T) are longer than those in Ni(η^2-T)$_2$, indicating a stronger bond in Ni(η^2-T)$_2$ than in Ni(η^5-T). Such a result implies that the energetic preference in the Ni−thiophene complex is for distorted tetrahedral coordination. The Co−C bonds adjacent to S−C bonds in Co(η^4-T) are longer than those in Co(η^2-T)$_2$, while the Co−C bonds away form the S−C bonds are slightly shorter.

3.2. Bonding Properties and Stability of Complexes. The bonding properties can be estimated by natural atom orbital bond order (NAO order) obtained from NBO calculation at B3LYP/6-31+G(d)//MPWB1K/6-311+G(d,p) basis set level, as shown in Table 1. The result of the bond order analysis shows a good agreement with the geometry. The S−C bond order in complexes is always smaller than that in free thiophene. In Fe(η^4-T)$_2$, Fe(η^4-T), Co(η^4-T), and Ni(η^5-T), the C=C bond order is weaker than that in free thiophene, and the C−C bond order is stronger. In Co(η^2-T)$_2$ and Ni(η^2-T)$_2$, the coordinated C=C and the C−C bonds show a weaker bond order than those in free thiophene. Clearly the complex formation weakens the relevant bonds in thiophene, as its electrons partially flow to the metal center. During the coordination, $C(sp^2)=C(sp^2)$ bond changes to $C(sp^3)-C(sp^3)$ and $S-C(sp^2)$ bond to $S-C(sp^3)$. It is noted that the coordination-induced bond order change occurs more on the C=C bond than on the S−C bond. The weakened S−C bond may play an important role during the bond cleavage,

TABLE 2: Bond Dissociation Enthalpies Computed at the B3LYP/6-31+G(d) Level in kcal/mol

	ΔH_1	ΔH_2	ΔH_3		ΔH_4	ΔH_5
Fe(η^4-T)$_2$	97.7	47.1	698.0	Fe(η^4-T)	51.3	240.4
Co(η^2-T)$_2$	35.4	28.5	712.1	Co(η^4-T)	9.0	291.7
Ni(η^2-T)$_2$	69.5	33.2	359.7	Ni(η^5-T)	33.1	193.9

which eventually leads to the desulfurization of thiophene or metal insertion into S−C bond.[12]

On the basis of the calculated bond order (Table 1), the M−C bond adjacent to S−C bond is stronger than those away from the S−C bond. The Fe−C bond in Fe(η^4-T) is stronger than that in Fe(η^4-T)$_2$. However, in the complexes of Co and Ni, the M−C bond in monothiophene complexes is weaker than that in bisthiophene complexes. Among monothiophene complexes, the observed M−C bond strength is on the order of Fe−C > Co−C > Ni−C bond.

To estimate the coordination stability, the enthalpies of homolytic or heterolytic dissociation (ΔH) of neutral complexes to M, MT, or M^{2+}, and T or T^-, are calculated at the B3LYP/6-31+G(d) level by the following equations:

The homolytic dissociation:

$$MT_2 \rightarrow M + 2T \qquad \Delta H_1 = (E_M + 2E_T) - E_{MT_2} + \Delta E_{cp} \quad \text{(i)}$$

$$MT_2 \rightarrow MT + T \qquad (\Delta H_2 = (E_{MT} + E_T) - E_{MT_2} + \Delta E_{cp} \quad \text{(ii)}$$

$$MT \rightarrow M + T \qquad (\Delta H_4 = (E_M + E_T) - E_{MT} + \Delta E_{cp} \quad \text{(iii)}$$

and the heterolytic dissociation:

$$MT_2 \rightarrow M^{2+} + 2T^- \qquad (\Delta H_3 = (E_{M^{2+}} + 2E_{T^-}) - E_{MT_2} + \Delta E_{cp} \quad \text{(iv)}$$

$$MT \rightarrow M^+ + T^- \qquad (\Delta H_5 = (E_{M^+} + 2E_{T^-}) - E_{MT} + \Delta E_{cp} \quad \text{(v)}$$

The dissociation enthalpies are listed in Table 2.

As expected, the heterolytic bond dissociation enthalpies of the complex are much larger than the corresponding homolytic ones. At the B3LYP/6-31+G(d) level of theory, calculated heterolytic dissociation enthalpy of the neutral Cp_2Fe to Fe^{2+} and $2Cp^-$ species is 702 kcal/mol (corresponding experimental value[46] is 662 kcal/mol), which is higher than that of Fe(η^4-T)$_2$ to Fe^{2+} and $2T^-$ species by only 4 kcal/mol. However, the homolytic dissociation enthalpy (97.7 kcal/mol) of Fe(η^4-T)$_2$ to Fe and 2T is much lower than that of $FeCp_2$ to Fe and 2Cp species (205 kcal/mol). Although the coordination of metal−thiophene is much weaker than that of metal−cyclopentadiene, there exists the typical metal coordination among thiophene complexes with Fe, Co and Ni. The Fe−thiophene coordination is stronger than the Co/Ni−thiophene one. The bisthiophene complexes of Co and Ni are apt to cleave homolytically to neutral monothiophene complexes and free thiophene, which prefer to adopt the conformation with the thiophene ligand in a η^4- or η^5-bonding mode.

The natural bond orbital (NBO) population calculation gives the net charge distributions before and after coordination. The results of charge redistribution show that the net natural charges on the metal center are 0.14, 0.74, 0.41, 0.61, 0.56, and 0.44 charge units for Fe(η^4-T)$_2$, Co(η^2-T)$_2$, Ni(η^2-T)$_2$, Fe(η^4-T), Co(η^4-T), and Ni(η^5-T), respectively. And the positive charges on S atom are decreased and the negative charges on C atoms are increased. As a result of the valence orbital interaction between thiophene and metals, the energy level of the highest occupied molecular orbital (HOMO) in the complexes is higher than that in free thiophene, and the energy level of the lowest unoccupied molecular orbital (LUMO) is lower (see Table 3). The metal complexation, therefore, greatly decreases the energy gap between the HOMO and LUMO orbitals. The changes of the frontier orbital energy level lead to the changes of molecular electrophilicity, which can be estimated by the electrophilicity index (ω) definited as[23,45]

$$\omega = \mu^2/2\eta$$

$$\mu = \frac{\varepsilon_{HOMO} + \varepsilon_{LUMO}}{2} \qquad \eta = \varepsilon_{LUMO} - \varepsilon_{HOMO}$$

where μ and η are the chemical potential and hardness, respectively. After coordination, complexes show more electrophilicity than free thiophene with an exception of Fe(η^4-T)$_2$. Moreover, the monothiophene complexes of Fe and Co have a higher electrophilicity than their bisthiophene complexes. The increase of molecular electrophilicity also implies that a charge transfer from ligand to metal (LMCT) occurs.

3.3. Analysis of Vibration Frequency and Simulation of Infrared Spectra. The analysis of harmonic vibration frequencies was performed on the basis of the equilibrium structures. Simulated infrared (IR) spectra were shown in Figure 2. The differences of characteristic absorption bands among complexes could help to identify and distinguish the respective compounds.

As shown in Figure 2a, the maximum absorption of Fe(η^4-T)$_2$ at 435.2 cm^{-1} is assigned to the ligand−Fe−ligand asymmetric stretching vibration mode along x axis direction. The second at 157.6 cm^{-1} is attributed to the S atom asymmetric stretching along $-x$ axis direction. Simulated IR spectra of Co(η^2-T)$_2$ and Ni(η^2-T)$_2$ are quite similar due to the similar coordinating mode. The maximum absorptions are all attributed to the out-of-plane vibration mode of C−H bonds, at 701.7 cm^{-1} for Co(η^2-T)$_2$ and at 699.3 cm^{-1} for Ni(η^2-T)$_2$, respectively. For Co(η^2-T)$_2$ and Ni(η^2-T)$_2$, the C−M−C asymmetric stretch vibration gives two bands, at 495.7 and 378.1 cm^{-1} for Co(η^2-T)$_2$ and at 467.9 and 383.8 cm^{-1} for Ni(η^2-T)$_2$, respectively, which can be found that such vibration bands in Co(η^2-T)$_2$ are slightly weaker than those in Ni(η^2-T)$_2$.

For the same metal, the maximum absorbing band in the monothiophene complexes shows a blue shift compared to that in the bisthiophene complexes, seeing Figure 2b. The first three strong absorption bands of Fe(η^4-T) at 848.4, 762.3, and 800.5 cm^{-1}, respectively, the first two absorption bands of Co(η^4-T) at 748.0 and 768.2 cm^{-1}, and the first three absorption bands of Ni(η^5-T) at 765.8, 731.4, and 685.6 cm^{-1}, respectively, are assigned to the out-of-plane vibration modes of C−H bonds. The M−S stretching vibration is in the far-infrared region. Hutchinson reported that the high spin (HS) of Fe−S bond stretching vibration appears at 205−250 cm^{-1}.[47,48] Our calculation indicates that the Fe−S bond stretching vibration in Fe(η^4-T) at 209.2 cm^{-1} is attributed to HS state. The Co−S bond

TABLE 3: Energy of Frontier Orbital (HOMO and LUMO) and the Electrophilicity (ω, eV) Computed at the B3LYP/6-31+G(d)//MPWB1K/6-311+G(d,p) Level

	Fe(η^4-T)$_2$	Co(η^2-T)$_2$	Ni(η^2-T)$_2$	Fe(η^4-T)	Co(η^4-T)	Ni(η^5-T)	T
HOMO	−5.13	−7.21	−6.01	−5.42	−6.00	−5.60	−7.56
LUMO	−0.24	−0.48	−0.51	−1.09	−1.02	−0.54	0.22
E_g	5.37	7.69	6.52	6.51	7.02	6.14	7.78
ω	0.738	1.097	0.964	1.221	1.235	0.931	0.866

stretching vibration at 155.8 cm^{-1} in Co(η^4-T) shows a weaker intensity than the Co−thiophene stretching vibration at 327.0 cm^{-1}. However, the Ni−S bond stretching vibration in Ni(η^5-T) at 150.0 cm^{-1} shows a stronger intensity than the Ni−thiophene stretching vibration at 309.0 cm^{-1}. The high-frequency band beyond 3000 cm^{-1} is assigned to the C−H stretching modes, with the low intensity.

3.4. Frontier Orbital Properties and Electronic Excited State Spectra. The electronic transition energies of the first ten singlet excited states for present systems were computed using TD-MPWB1K method with the 6-311+G(d,p) basis set level. Theoretical electronic absorption spectra based on the excited state (n, $n = 10$) versus the oscillator strength (f) were simulated and shown in Figure 3. The corresponding frontier orbitals significantly contributing to the electronic transition were drawn in Figure 4.

As expected, the complexes reveal a large red shift in the maximum absorption in comparison with that of free thiophene. For the bisthiophene complexes of Fe and Ni, the maximum peaks are in the near-ultraviolet area. The absorption maxima of Co(η^2-T)$_2$, Fe(η^4-T), Co(η^4-T), and Ni(η^5-T) are in the visible region. For the same metal, the absorption maxima of monothiophene complexes are red-shifted by more than 12.40 eV in comparison with those of the bisthiophene ones, accompanied by a large decrease in intensity. It can be seen that the absorbing strength of the bisthiophene complexes is stronger than that of the free thiophene. Among bisthiophene complexes, the maximum absorption of Ni(η^2-T)$_2$ shows a much larger intensity than those of Fe(η^4-T)$_2$ and Co(η^2-T)$_2$.

Calculated maximum absorption of free thiophene at 6.05 eV is assigned to the electronic lowest-lying excitation transition from HOMO to LUMO, which is overestimated by about 0.70 eV in comparison with the experimental one.[20] However, the absorption maxima of complexes are not attributed to the HOMO → LUMO transition. The maximum absorption of Fe(η^4-T)$_2$ at 3.54 eV is assigned to the electronic transition from HOMO−4 that is mainly composed of the 4s orbital of Fe mixing with its 3d$_{z^2}$ and 3d$_{x^2-y^2}$ orbitals and the π-type antibonding orbital of thiophene, to the LUMO that is mainly composed of the 4s, 4p$_x$, and 4p$_y$ orbitals of Fe and the π-type antibonding orbital of ligand. The next transition at 3.30 eV is assigned to the transition from HOMO that is mainly composed of the 3d$_{xy}$ and 3p$_x$ orbitals of Fe and the π-type bonding orbitals of thiophene ligand, to LUMO+3 that is chiefly dominated by the 4p$_x$ orbital of Fe and the π-type antibonding orbital of ligand.

The maximum absorption of Co(η^2-T)$_2$ at 1.64 eV is assigned to the electronic transition from HOMO−2 to LUMO+1. The HOMO−2 orbital is dominantly composed of π-type bonding orbitals of thiophene ligand, and LUMO+1 is dominantly composed of π-type antibonding orbital of ligand in addition with the 4p$_z$ and 3d$_{xy}$ orbitals of Co. Interestingly, the second transition of HOMO−1 → HOMO at 1.37 eV is ascribed to the transition from the 3d$_{xz}$ orbital (HOMO−1) of Co to the singly occupied HOMO (SOMO) dominated by 3p$_x$ orbital of S atom. The 3d$_{xz}$ electrons of Co can be excited to the higher virtual orbital (LUMO+13) at the energy of 2.15 eV.

The maximum absorptions of Ni(η^4-T)$_2$ at 3.83 eV include two doubly degenerate transitions from HOMO−1 to LUMO+2 and from HOMO−2 to LUMO+2, respectively. The HOMO−1 orbital is mainly composed of the 3d$_{xy}$ and 4s orbitals of Ni and the 3p$_x$ of S atom. The HOMO−2 orbital is mainly composed of the 3d$_{z^2}$ and 4s orbitals of Ni mixing with the 3d$_{xz}$ orbital. LUMO+2 orbital is dominated by the 4p$_x$ and 4p$_z$ orbitals of Ni mixing with the negligible contribution from 3d$_{xy}$ orbitals of Ni. The HOMO of Ni(η^2-T)$_2$ is constructed from the π-type bonding orbitals of ligand and the 3d$_{xy}$ orbitals of Ni, and the LUMO is composed of the π-type antibonding orbital of ligand and the 4s and 3d$_z^2$ orbitals of Ni. The HOMO → LUMO transition absorption is the second band.

For monothiophene complexes, the transition from HOMO to LUMO is the forbidden transition. The maximum absorption at 2.75, 1.43, and 2.58 eV for Fe(η^4-T), Co(η^4-T), and Ni(η^5-T) is assigned to the HOMO−1 → LUMO transition, HOMO−1 → HOMO transition, and HOMO−1 → LUMO transition,

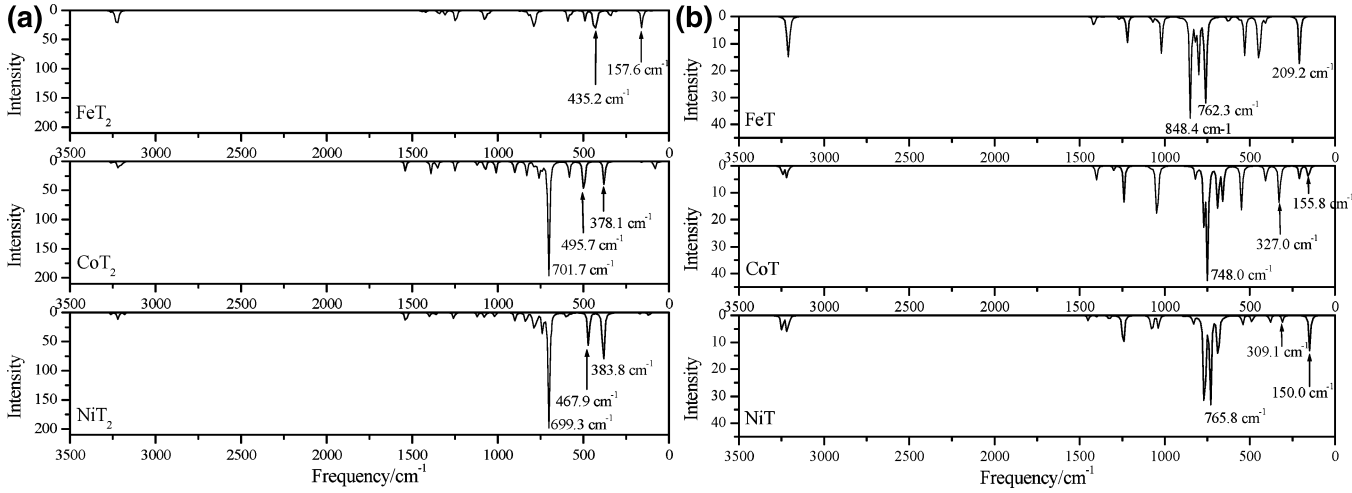

Figure 2. Simulated IR for (a) MT$_2$ and (b) MT at the B3LYP/6-31+G(d) level, T = thiophene, M = Fe, Co, Ni.

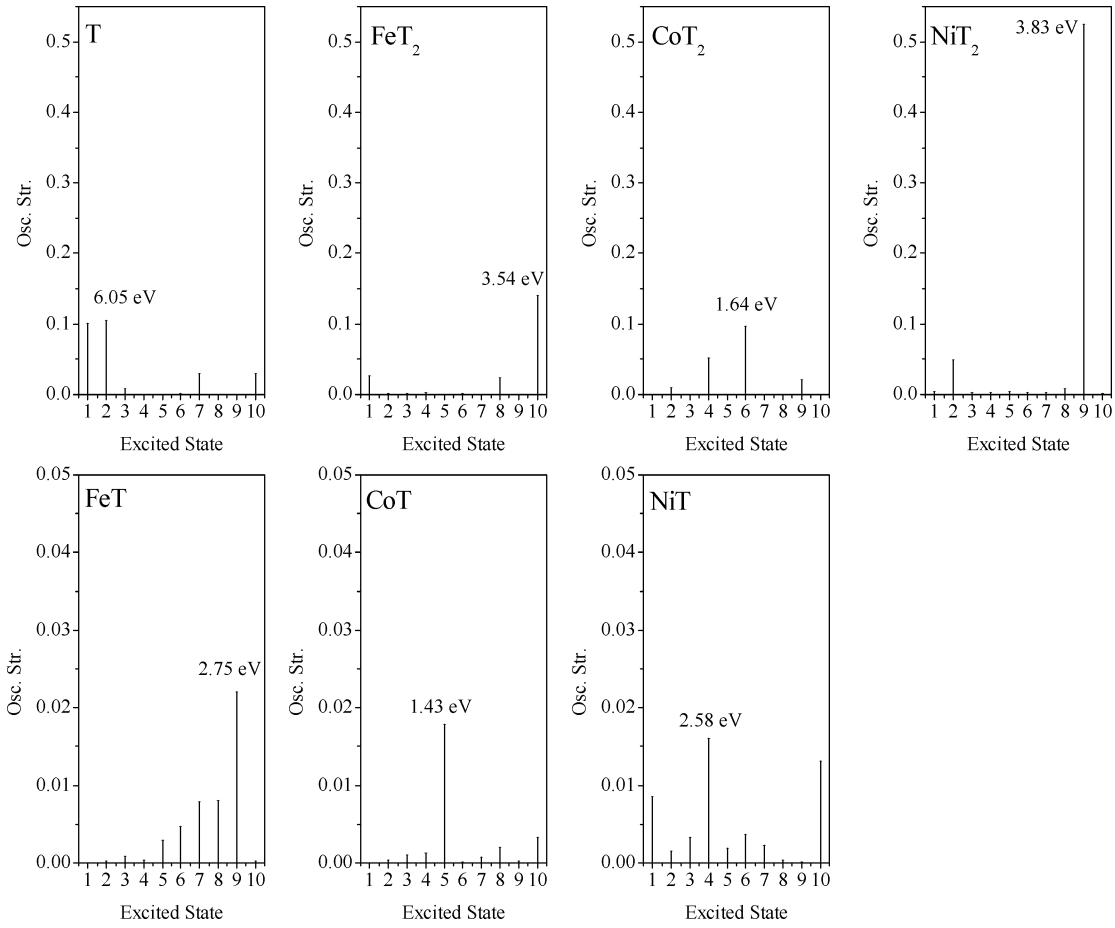

Figure 3. Calculated electron-excited state sepctra of MT_2 and MT at the TD-MPWB1K/6-311+G(d,p) level. The data are the maximum excited energy in eV.

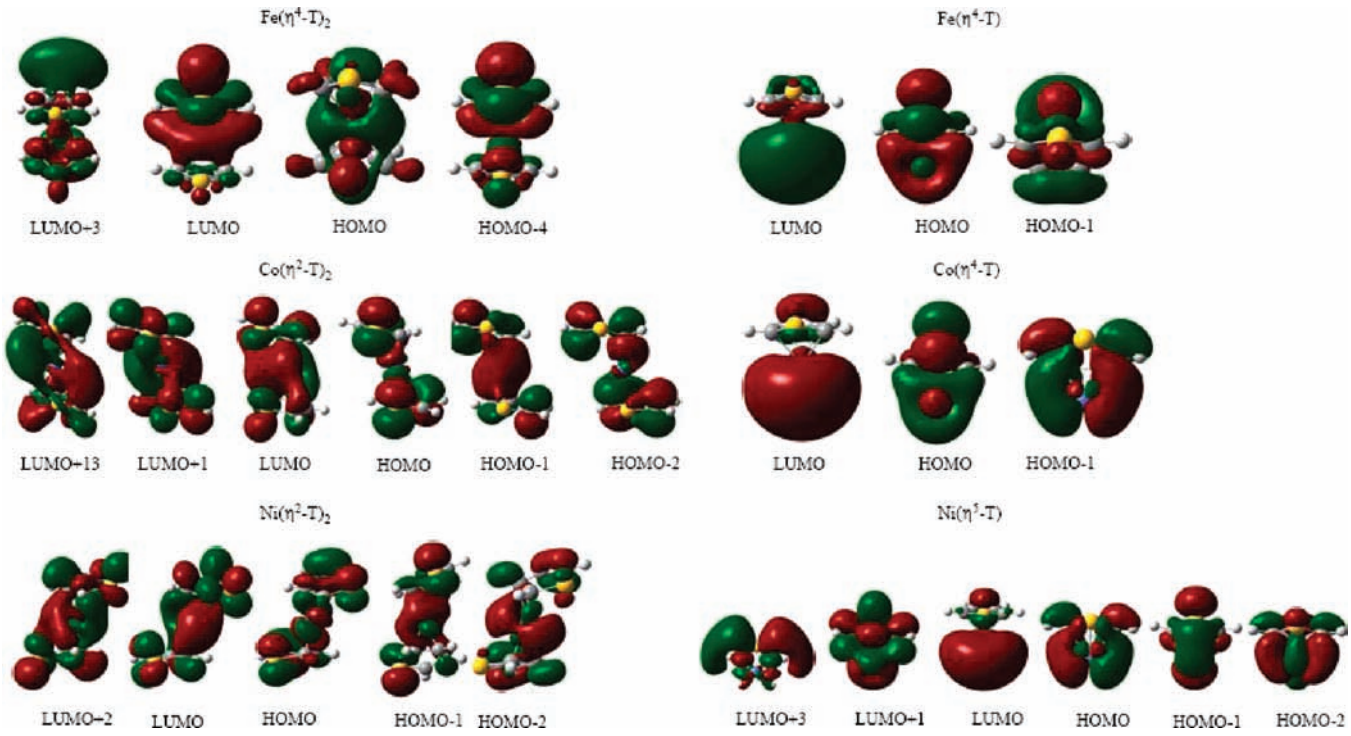

Figure 4. Frontier molecular orbital significantly contributing to the electronic transition molecules.

respectively. The HOMO−1 orbital of Fe(η^4-T) is a metal−ligand interaction orbital mainly composed of the d-type orbital ($3d_{xz}$ and $3d_{x^2-y^2}$) and π-type bonding orbital of ligand, and LUMO is dominanted by the 4s orbital of Fe mixing with its $4p_x$ and $4p_z$ orbitals. The maximum transition of Co(η^4-T) is from the π-type metal−ligand bonding orbital to the single occupied $3d_{z^2}$

orbital of Co. The maximum transition of Ni(η^5-T) is from nonbonding d-type orbitals ($3d_{x^2-y^2}$ and $3d_{xy}$) of Ni to its antibonding 4s orbital. The next transition at 3.76 eV contains two degenerate transition from the HOMO−2 to LUMO+1, and from the HOMO to LUMO+3, respectively. The HOMO−2 and HOMO are the bonding Ni−ligand interaction orbitals constructed from the π-type orbital of ligand and the d-type orbitals ($3d_{z^2}$, $3d_{xy}$, $3d_{xz}$, $3d_{x^2-y^2}$) of Ni. The LUMO and LUMO+1 are corresponding antibonding orbitals.

4. Conclusions

A DFT study has been performed on the thiophene complexes with Fe, Co, and Ni, which gives insight into the property of the electronic structure of complexes that is difficult to obtain by the experiment, including geometrical structures, bonding properties, and spectroscopic properties.

The equilibrium geometries show the η^4-bonding mode of the thiophene ligand for Fe(η^4-T)$_2$, Fe(η^4-T), and Co(η^4-T), η^2-bonding mode for Co(η^2-T)$_2$ and Ni(η^2-T)$_2$, and η^5-bonding mode for Ni(η^5-T), respectively. The complexes of Fe have the strongest coordination stability among the present systems, which put forward a workable idea that one-dimensional thiophene-based supermolecuar architecture could be constructed from the thienyl-bridged complexes with Fe. The frequency calculation clearly shows the thiophene−metal−thiophene asymmetric vibration absorption with a strong intensity, at 435.2, 495.7, and 383.1 cm^{-1} for Fe(η^4-T)$_2$, Co(η^2-T)$_2$, and Ni(η^2-T)$_2$, respectively. And the M−S stretching vibration of monothiophene complexes has a significant absorption in the far-infrared region, at 209.2, 155.8, and 150.0 cm^{-1} for Fe(η^4-T), Co(η^4-T), and Ni(η^5-T), respectively. The electronic absorption maxima of the bisthiophene complexes exhibit a greater blue shift in comparison with the monothiophene ones. Except that the maximum absorption bands of the bisthiophene complexes of Fe and Ni are in near-ultraviolet area, the absorption maxima of Co(η^2-T)$_2$, Fe(η^4-T), Co(η^4-T) and Ni(η^5-T) are in the visible region. The calculated result suggests an advisible method to recognize the thiophene-based species by the discernible spectral properties of the metal complexation.

Acknowledgment. We are indebted to Dr. Yi Pang for his help with the paper. This work was supported by the National Natural Science Foundation of China (Nos. 20574043, 20874057, 20877049), the Key Natural Science Foundation of Shandong Province of China (No. Z2007B02).

Supporting Information Available: Significant vibration modes based on the analysis of vibrational frequencies computed at the B3LYP/6-31+G(d) level of theory (Schemes 1−6). Selected structural parameters of equilibrium geometries for bis- and monothiophene complexes (Table 1*). Calculated excitation energies (in eV) with $f \geq 0.01$ in the first ten electronical excited states at MPWB1K/6-311+G(d,p) basis set level and transition orbitals with the largest coefficients (Table 2*). This material is available free of charge via the Internet at http://pubs.acs.org.

References and Notes

(1) Huckett, S. C.; Sauer, N. N.; Angelici, R. J. *Organometallics* **1987**, *6*, 591.
(2) Angelici, R. J. *Acc. Chem. Res.* **1988**, *21*, 387.
(3) Angelici, R. J. *Acc. Chem. Res.* **1988**, *105*, 61.
(4) Benson, J. W.; Angelici, R. J. *Organometallics* **1992**, *11*, 922.
(5) Reynolds, M. A.; Guzei, I. A.; Logsdon, B. C.; Thomas, L. M.; Jacobson, R. A.; Angelici, R. J. *Organometallics* **1999**, *18*, 4075.
(6) Liang, Z.; Thomas, C. W. Mak. *Organometallics* **2007**, *26*, 4439.
(7) Liang, Z.; Thomas, C. W. Mak. *J. Am. Chem. Soc.* **2005**, *127* (43), 14966.
(8) Hisashi, K.; Wu, L. P; Megumu, M.; Takayoshi, K. S.; Masahiko, M.; Yusaku, S. *Inorg. Chem.* **2003**, *42*, 1928.
(9) Wang, Q. M.; Thomas, C. W. Mak. *Inorg. Chem.* **2003**, *42* (5), 1637.
(10) Zang, S. Q.; Thomas, C. W. Mak. *Inorg. Chem.* **2008**, *47* (16), 7094.
(11) Ryuhei, U.; Hiroshi, A.; Tsukasa, N.; Hisashi, F. *J. Am. Chem. Soc.* **2008**, *130*, 3240.
(12) Angelici, R. J. *Organometallics* **2001**, *20* (7), 1259.
(13) Benson, J. W.; Angelici, R. J *Organometallics* **1993**, *12* (3), 680.
(14) Coleman, A.; Pryce, M. T. *Inorg. Chem.* **2008**, *47* (23), 10980.
(15) Djukic, B.; Dube, P. A.; Razavi, F.; Seda, T.; Jenkins, H. A.; Britten, J. F.; Lemaire, M. T. *Inorg. Chem.* **2009**, *48* (2), 699.
(16) Wen, H.; Cao, M. H.; Sun, G. B.; Xu, W. G.; Wang, D.; Zhang, X. Q.; Hu, C. W *J. Phys. Chem. C* **2008**, *112* (41), 15948.
(17) Layman, K. A.; Bussell, M. E. *J. Phys. Chem. B* **2004**, *108* (40), 15791.
(18) Hu, H. R.; Qiao, M. H.; Xie, F. Z.; Fan, K. N.; Lei, H.; Tan, D. L.; Bao, X. H.; Lin, H. L.; Zong, B. N.; Zhang, X. X. *J. Phys. Chem. B* **2005**, *109*, 5186.
(19) Betteridge, D. *Anal. Chem.* **1972**, *44* (5), 100.
(20) Šolc, R.; Lukeš, V.; Klein, E.; Griesser, M.; Kelterer, A. M. *J. Phys. Chem. A* **2008**, *112*, 10931.
(21) Linares, M.; Scifo, L.; Demadrille, R.; Brocorens, P.; Beljonne, D.; Lazzaroni, R.; Grevin, B. *J. Phys. Chem. C* **2008**, *112*, 6850.
(22) Heejoon, A.; James, E. W. *J. Phys. Chem. B* **2003**, *107*, 6565–6572.
(23) Athanassios, C. T.; Aikaterini, Th. C. *Inorg. Chem.* **2004**, *43*, 1273–1286.
(24) Lein, M.; Frunzke, J.; Frenking, G. *Inorg. Chem.* **2003**, *42*, 2504–2511.
(25) Becke, A. D. *Phys. Rev. A* **1988**, *38*, 3098.
(26) Lee, C.; Yang, W.; Parr, R. G. *Phys. Rev. B* **1988**, *37*, 785.
(27) Miehlich, B.; Savin, A.; Stoll, H.; Preuss, H. *Chem. Phys. Lett.* **1989**, *157*, 200.
(28) Stephens, P. J.; Devlin, F. J.; Ashvar, C. S.; Chabalowski, C. F.; Frisch, M. J. *Faraday Discuss.* **1994**, *99*, 103.
(29) Stephens, P. J.; Devlin, F. J.; Frisch, M. J.; Chabalowski, C. F. *J. Phys. Chem.* **1994**, *98*, 11623.
(30) Ren, G. M.; Li, S. D.; Miao, C. Q. *J. Mol. Struct. (THEOCHEM)* **2006**, *770*, 193.
(31) Feng, S. Y.; Feng, D. C.; Li, M. J.; Zhou, Y. F.; Wang, P. G. *J. Mol. Struct.(THEOCHEM)* **2002**, *618*, 51.
(32) Simon, S.; Duran, M.; Dannenberg, J. J. *J. Chem. Phys.* **1996**, *105*, 11024.
(33) Boys, S. F.; Bernardi, F. *Mol. Phys.* **1970**, *19*, 553.
(34) Liao, M. S.; Watts, J. D.; Huang, M. J. *J. Phys. Chem. B* **2007**, *111*, 4374.
(35) Rao, J. S.; Sastry, G. N. *J. Phys. Chem. A* **2009**, *111*, 4374.
(36) Reed, A. E.; Curtiss, L. A.; Weinhold, F. *Chem. Rev.* **1988**, *88*, 899.
(37) Weinhold, F.; Carpenter, J. E. *Plenum* **1988**, 227.
(38) Carpenter, J. E.; Weinhold, F. *J. Mol. Struct. (THEOCHEM)* **1988**, *169*, 41.
(39) Wodrich, M. D.; Corminboeuf, C.; Schreiner, P. R.; Fokin, A. A.; Ragué Schleyer, P. *Org. Lett.* **2007**, *9* (10), 1851.
(40) Zhao, Y.; Truhlar, D. G. *J. Chem. Theory Comput.* **2007**, *3* (1), 289.
(41) Bauernschmitt, R.; Ahlrichs, R. *Chem. Phys. Lett.* **1996**, *256*, 454.
(42) Casida, M. E.; Jamorski, C.; Casida, K. C.; Salahub, D. R. *J. Chem. Phys.* **1998**, *108*, 4439.
(43) Stratmann, R. E.; Scuseria, G. E.; Frisch, M. J. *J. Chem. Phys.* **1998**, *109*, 8218.
(44) Frisch, M. J.; Trucks, G. W.; Schlegel, H. B.; Scuseria, G. E.; Robb, M. A.; Cheeseman, J. R.; Montgomery, J. A., Jr.; Vreven, T.; Kudin, K. N.; Burant, J. C.; Millam, J. M.; Iyengar, S. S.; Tomasi, J.; Barone, V.; Mennucci, B.; Cossi, M.; Scalmani, G.; Rega, N.; Petersson, G. A.; Nakatsuji, H.; Hada, M.; Ehara, M.; Toyota, K.; Fukuda, R.; Hasegawa, J.; Ishida, M.; Nakajima, T.; Honda, Y.; Kitao, O.; Nakai, H.; Klene, M.; Li, X.; Knox, J. E.; Hratchian, H. P.; Cross, J. B.; Adamo, C.; Jaramillo, J.; Gomperts, R.; Stratmann, R. E.; Yazyev, O.; Austin, A. J.; Cammi, R.; Pomelli, C.; Ochterski, J. W.; Ayala, P. Y.; Morokuma, K.; Voth, G. A.; Salvador, P.; Dannenberg, J. J.; Zakrzewski, V. G.; Dapprich, S.; Daniels, A. D.; Strain, M. C.; Farkas, O.; Malick, D. K.; Rabuck, A. D.; Raghavachari, K.; Foresman, J. B.; Ortiz, J. V.; Cui, Q.; Baboul, A. G.; Clifford, S.; Cioslowski, J.; Stefanov, B. B.; Liu, G.; Liashenko, A.; Piskorz, P.; Komaromi, I.; Martin, R. L.; Fox, D. J.; Keith, T.; Al-Laham, M. A.; Peng, C. Y.; Nanayakkara, A.; Challacombe, M.; Gill, P. M. W.; Johnson, B.; Chen, W.; Wong, M. W.; Gonzalez, C.; Pople, J. A. *Gaussian 03*, revision B.03; Gaussian, Inc.: Pittsburgh, PA, 2003.

(45) Parr, R. G.; Szentpály, L. v.; Liu, S. *J. Am. Chem. Soc.* **1999**, *121*, 1922.
(46) Ryan, M. F.; Eyler, J. R.; Richardson, D. E. *J. Am. Chem. Soc.* **1992**, *114*, 8611.
(47) Sonal, S.; Garg, A. N.; Kailash, C. *J. Alloys Compd.* **2007**, *443*, 53.
(48) Hutchinson, B.; Neill, P.; Finkelstein, A.; Takemoto, J. *Inorg. Chem.* **1981**, *20*, 2000.

JP902920W